Peripheral CB1R inhibition modulates food intake and metabolic efficiency in obesity independently of the gut-brain vagal axis

Oriane Onimus[1], Camille de Almeida[1,*], Benoit Bertrand[1,*], Julien Castel[1], Anthony Ansoult[1], Serge Luquet[1], Giuseppe Gangarossa[1,2]

[1] Université Paris Cité, CNRS, Unité de Biologie Fonctionnelle et Adaptative, F-75013 Paris, France.

[2] Institut Universitaire de France (IUF)

* These authors contributed equally

Correspondence should be address to: giuseppe.gangarossa@u-paris.fr (G.G.)

Key words: peripheral CB1 receptor, gut-brain axis, vagus nerve, brainstem, feeding behavior

Abstract

Obesity arises from profound disruptions in neuroendocrine communication and impaired central regulation of energy homeostasis. The endocannabinoid system (ECS), through cannabinoid type-1 receptors (CB1Rs), is a key modulator of feeding, metabolism, and gut-brain signaling. While global CB1R blockade improves metabolic control, its clinical translation has been limited by adverse neuropsychiatric effects, underscoring the therapeutic potential of peripherally restricted CB1R inhibition whose neural mechanisms remain insufficiently defined. Here, we show that two peripheral CB1R antagonists, the inverse agonist JD-5037 and the neutral antagonist AM6545, selectively suppress food intake and shift nutrient partitioning toward fat oxidation in obese, but not lean, mice, without altering total energy expenditure. We further demonstrate that high-fat exposure markedly upregulates CB1R expression in the nodose ganglia, suggesting an enhanced reliance on periphery-to-brain ECS signaling in obesity.

Using cFos mapping, we reveal that inhibition of peripheral CB1Rs robustly recruits satiety-related brainstem and hypothalamic structures. Interestingly, disruption of the gut-brain vagal axis abolishes JD-5037-induced activation of brainstem nuclei but leaves hypothalamic activation, and the anorexigenic response, fully intact. Likewise, pharmacological inhibition of key vagal endocrine mediators, cholecystokinin (CCK) and glucagon-like peptide-1 (GLP-1), fails to blunt the feeding-suppressive effects of peripheral CB1R blockade.

These findings uncover an unprecedent dual mechanism whereby vagal pathways mediate brainstem engagement, whereas hypothalamic recruitment and metabolic benefits arise through vagal-independent signaling. Our results position peripheral CB1R inhibition as a mechanistically distinct approach capable of engaging central homeostatic circuits without direct brain penetration, supporting peripherally acting CB1R antagonists as promising therapeutics for obesity and metabolic disorders.

Introduction

Obesity is a multifactorial metabolic disease characterized by a chronic positive energy balance, altered eating patterns, excessive fat accumulation, and systemic metabolic dysfunctions. It is associated with increased risks of type 2 diabetes, cardiovascular disease, non-alcoholic fatty liver disease, and several cancers. Growing evidence suggests that obesity may be initiated and/or worsened by distorted functioning of neuronal ensembles as well as of altered body-brain communications [1,2]. However, despite intense research efforts, long-term non-invasive and efficient therapies remain limited, primarily due to the complexity of the underlying regulatory networks that govern energy homeostasis. Among these networks, the endocannabinoid system (ECS) has emerged as a key modulator of both central and peripheral neuronal mechanisms that control appetite, energy storage, glucose metabolism, and lipid homeostasis [3,4].

The ECS consists of endogenous cannabinoids [*i.e.,* anandamide (AEA) and 2-arachidonoylglycerol (2-AG)], their receptors [cannabinoid receptor type 1 (CB1R) and type 2 (CB2R)] and the enzymes responsible for their synthesis and degradation. While the role of centrally expressed CB1R in regulating feeding behavior and hedonic aspects of food intake is well-established [3–5], there is a growing recognition that CB1 receptors located in peripheral tissues (*i.e.,* adipose tissue, liver, muscles, peripheral nervous system and gastrointestinal tract) also contribute to metabolic dysfunctions and represent promising anti-obesity targets [4,6]. In particular, CB1R activation in peripheral organs promotes lipogenesis, impairs insulin sensitivity, and alters gastrointestinal motility and secretion, whereas CB1R inhibition/blockade counteracts such effects [7,8]. This therapeutic potential of leveraging the ECS is supported by both clinical and preclinical studies demonstrating elevated levels of AEA and/or 2-AG in several eating disorders [9–12] and also in obesity [13–15], therefore suggesting a constant overactivation of the ECS system in these conditions.

Early pharmacological approaches targeting the ECS, such as the use of rimonabant, a centrally and peripherally active CB1R inverse agonist, demonstrated robust metabolic improvements and weight loss in obese individuals [16]. However, these benefits were overshadowed by significant neuropsychiatric side effects, including anxiety and depression [17–19], due to CB1R antagonism in the brain. This led to the development of peripherally restricted CB1R antagonists and inverse agonists that do not cross the blood-brain barrier [7,8,20,21]. Preclinical studies using such compounds have shown promising effects, including reduction in body

weight, improved glucose tolerance, enhanced thermogenesis, and decreased hepatic steatosis, all without eliciting central side effects [7,8,20–24].

An area of active investigation is the extent to which the metabolic and behavioral benefits of peripheral CB1R inhibition are mediated by specific organs [25–28] and also the gut-brain axis [9,29], particularly via the vagal signaling. The vagus nerve serves as a crucial bidirectional conduit between the gut and the brain, transmitting nutritional, hormonal, and microbial signals to central circuits that regulate appetite and metabolism. Peripheral CB1Rs are expressed along the gut epithelium [30,31] as well as in afferent/sensory vagal neurons [9,29,32,33] raising the possibility that pharmacological modulation of CB1R may recruit vagal-dependent mechanisms to influence systemic metabolism.

However, whether the metabolic improvements observed with peripheral CB1R antagonism in obesity are entirely dependent on an intact gut-brain vagal pathway remains unclear. Distinguishing vagus nerve-dependent from vagus nerve-independent mechanisms is essential for optimizing the therapeutic potential of peripheral CB1R inhibition/blockade and understanding its full range of physiological effects. Furthermore, clarification of these mechanisms could broaden the scope of CB1R-targeted therapies to patient populations with altered or impaired vagal signaling.

In this study, we investigated whether and how peripheral CB1R inhibition influences energy metabolism under both physiological and pathological conditions, such as obesity. Our findings demonstrate that: (*i*) peripheral CB1R inhibition modulates energy metabolism in obese, but not lean, states; (*ii*) this modulation involves activation of brainstem and hypothalamic nuclei through both vagus-dependent and vagus-independent mechanisms respectively; and (*iii*) critically, the beneficial metabolic effects persist even in the absence of intact gut-brain vagal signaling. These results advance our understanding of endocannabinoid system modulation in metabolic diseases and support the need for continued development of peripherally restricted CB1R-targeted therapies as potentially safe and effective treatments for obesity and eating disorders.

Material and methods

Animals

All experimental procedures were approved by the Animal Care Committee of the Université Paris Cité (CEB-22-2019, APAFiS #24407; CEB-38-2021, APAFiS #35447), and carried out following the 2010/63/EU directive. 8-12 weeks old C57BL/6J male mice (Janvier, France) were used and housed in a room maintained at 22 ±1 °C, with a light period from 7h00 to 19h00. Regular chow diet (3.24 kcal/g, reference SAFE® A04, Augy, France), high-fat diet (HFD, Research Diets, Cat #D12492, 5.24 kcal/g) and water were provided *ad libitum* unless otherwise stated. All procedures were designed to minimize animal suffering and reduce the number of animals used.

Subdiaphragmatic vagotomy (SDV)

Prior to surgery and during 4-5 post-surgery days, animals were provided with *ad libitum* jelly food (DietGel Boost #72-04-5022, Clear H2O). Animals received Buprécare® (buprenorphine 0.3 mg/kg) and Ketofen® (ketoprofen 10 mg/kg) and were anaesthetized with isoflurane (3.5% for induction, 1.5% for maintenance). During surgery the body temperature was maintained at 37 °C using a heated pad. Briefly, using a binocular microscope, the right and left subdiaphragmatic branches of the vagus nerve were carefully isolated along the lower esophagus/stomach and carefully sectioned in vagotomized animals (SDV mice) or left intact in Sham animals. Mice recovered for at least 3-4 weeks before being used for experimental procedures. The efficiency of the SDV procedure was evaluated as previously described [9,34].

Drugs

Mice were administered with the following drugs: JD-5037 (3, 6, 10 mg/kg; #HY-18697, CliniSciences), AM6545 (3 mg/kg; # 5443, Tocris), Devazepide (0.3 mg/kg; #2304, Tocris), Exendin-(9-39) (0.1 mg/kg; #2081, Tocris) and respective vehicle solutions. JD-5037 and AM6545 were dissolved in a solution containing DMSO, Kolliphor and saline at the following ratio 2:1:97. Matched vehicles (saline or DMSO/Kolliphor/saline) were administered. Devazepide and Exendin-(9-39) were dissolved in saline. All drugs were injected in 10 mL/kg of body volume.

Tissue preparation and immunofluorescence

142 Mice were anaesthetized with pentobarbital (500 mg/kg, Dolethal, Vetoquinol, France) and
143 transcardially perfused with cold (4 °C) PFA 4% for 5 min. Brains were post-fixed in PFA 4%
144 at 4°C for 24h and changed in PBS 1X. 40 µm coronal sections were processed using a
145 vibratome (Leica). Confocal imaging acquisitions were performed after immunohistochemistry
146 protocol, using a confocal microscope (Zeiss LSM 710) as previously described [35,36]. The
147 following primary antibodies were used: rabbit anti-cFos (1:1000, Synaptic Systems, #226 003,
148 1:1000, Cell Signaling, #2250). Sections were incubated for 60 min with the following
149 secondary antibodies: donkey anti-rabbit Cy3 AffiniPure (1:1000, Jackson Immunoresearch,
150 711-165-152). Structures were selected according to the following coordinates (from bregma,
151 in mm): PBN (-5.02 to -5.34), AP/NTS (-7.32 to -7.76), PVN (-0.82 to -1.06) and ARC (-1.46
152 to -1.94). The objectives (10X or 20X) and the pinhole setting (1 airy unit) remained unchanged
153 during the acquisition of a series for all images. Quantification of immunopositive cells was
154 performed using the cell counter plugin of ImageJ taking a fixed threshold of fluorescence as
155 standard reference.
156
157 **Quantitative RT-PCR**
158 The nodose ganglia were dissected and snap-frozen using liquid nitrogen. All tissues were kept
159 at -80 °C until RNA extraction. Tissues were homogenized in TRIzol/QIAzol Lysis Reagent
160 (Life Technologies) with 3 mm tungsten carbide beads by using the Tissue Lyser III (QIAGEN,
161 9003240). Total RNA was extracted using the Rneasy Micro Kit (QIAGEN, 74004). The RNA
162 was quantified by using the NanoDrop 1000 spectrophotometer. 500 ng of mRNA from each
163 sample was used for retrotranscription, performed with the SuperScript®III Reverse
164 Transcriptase (Life Technologies) following the manufacturer's instructions. Quantitative RT-
165 PCRs were performed in a LightCycler 1.5 detection system (Roche, Meylan France) using the
166 Takyon No Rox SYBR MasterMix dTTP Blue (Eurogentec) in 384-well plates according to the
167 manufacturer's instruction. The following primers were used: *Cnr1* (forward 5'-3'
168 AGCAAGGACCTGAGACATG, reverse 5'-3': TGTTATTGGCGTGCTTGTGC), *Rpl19*
169 (forward 5'-3': GGGCAGGCATATGGGCATA; reverse 5'-3':
170 GGCGGTCAATCTTCTTGGATT). Relative concentrations were extrapolated from the
171 concentration range for each gene. Concentration values were normalized to the house-keeping
172 gene RPL19.
173
174 **Metabolic efficiency analysis**

Indirect calorimetry was performed as previously described [9,37]. Mice were monitored for whole energy expenditure (EE), O_2 consumption, CO_2 production, respiratory exchange rate (RER=VCO_2/VO_2, V=volume), fatty acid oxidation and locomotor activity using calorimetric cages (Labmaster, TSE Systems GmbH, Bad Homburg, Germany). Ratio of gases was determined through an indirect open circuit calorimeter. This system monitors O_2 and CO_2 at the inlet ports of a tide cage through which a known flow of air is ventilated (0.4 L/min) and regularly compared to a reference empty cage. O_2 and CO_2 were recorded every 15 min during the entire experiment. EE was calculated using the Weir equation for respiratory gas exchange measurements. Food intake was measured with sensitive sensors for automated online measurements. Mice were monitored for body weight and composition at the entry and exit of the experiment using an EchoMRI (Whole Body Composition Analyzers, EchoMRI, Houston, USA). Data analysis was performed on Excel XP using extracted raw values of VO_2, VCO_2 (ml/15 min), and EE (kcal/15 min).

Re-clustering and transcriptomics meta-analysis

Publicly available transcriptomic data [38] were downloaded from Gene Expression Omnibus (https://www.ncbi.nlm.nih.gov/geo/, GSE138651) and analyzed using a Python 3.0 pipeline generated in line with the original publication.

Statistics

All data are presented as mean ± SEM. Statistical tests were performed with Prism 10 (GraphPad Software, La Jolla, CA, USA). Depending on the experimental design, data were analyzed using either Student's t-test with equal variances, one-way ANOVA or two-way ANOVA. The significance threshold was automatically set at $p<0.05$. ANOVA analyses were followed by Bonferroni *post hoc* test for specific comparisons only when overall ANOVA revealed a significant difference (at least $p<0.05$).

Results

The metabolic efficacy of peripheral CB1R inhibition depends on the metabolic state

Recent studies have shown that pharmacological blockade/inhibition of peripheral CB1 receptors using agents such as JD-5037 or AM6545 holds strong promise for treating metabolic and eating disorders [for review see [39]]. Here, we explored whether and how peripheral CB1R inhibition affects feeding behavior and metabolic efficiency. To address this, we first administered different doses of the peripherally restricted CB1R inverse agonist JD-5037 (3, 6, and 10 mg/kg, i.p.) to lean mice fed a standard chow diet (CD) and assessed various metabolic parameters of energy homeostasis. Interestingly, JD-5037 had no significant effect on food intake (**Fig. 1A, E, I**), respiratory exchange ratio (**Fig. 1B, F, J**), fatty acid oxidation (**Fig. 1C, G, K**), or energy expenditure (**Fig. 1D, H, L**), compared to vehicle-treated controls. This set of results indicate that inhibition of peripheral CB1R in lean animals does not alter feeding, nutrient partitioning (oxidation of carbohydrates *versus* lipids) or energy balance.

Next, we investigated whether the beneficial effects of peripheral CB1R antagonism/inhibition depended on the metabolic state. Mice were fed a high-fat diet (HFD) for 2-3 months, leading to a significant increase in body weight (**Fig. 2A**). In contrast to lean mice, administration of the peripheral CB1R inverse agonist JD-5037 (3 mg/kg, i.p.) markedly reduced food intake in HFD-fed mice (**Fig. 2B, B^1**). This was accompanied by a shift in nutrient utilization favoring lipids over carbohydrates, as evidenced by a decreased respiratory exchange ratio (RER; **Fig. 2C, C^1**) and an increased fatty acid oxidation (FAO; **Fig. 2D, D^1**). These metabolic changes occurred without significant alterations in energy expenditure (EE; **Fig. 2E, E^1**) or spontaneous locomotor activity (**Fig. 2F**). Beside the metabolic state (chow diet- *versus* HFD-mice), we also wondered whether the nutritional state (fasted *versus* fed mice) may condition the anorexigenic effect of JD-5037. Again, we observed that JD-5037 (3 mg/kg) maintained its anorexigenic properties only in HFD-mice (food consumed after 4 hours of refeeding, **Fig. 2G**).

To further complement these findings, we used the peripherally restricted neutral CB1R antagonist AM6545 (3 mg/kg, i.p.) and observed comparable outcomes: a reduction in food intake (**Fig. 2H**) and a shift in nutrient partitioning (**Fig. 2I**), again without affecting energy expenditure (**Fig. 2J**).

Inhibition of peripheral CB1R activates satietogenic brainstem nuclei in a metabolic state-dependent manner via the gut-brain vagal axis

234 Building on our findings related to feeding behavior and energy metabolism, we next examined
235 whether peripheral CB1R inhibition triggers specific patterns of neuronal activation in key
236 brainstem nuclei involved in satiety regulation, namely the nucleus tractus solitarius (NTS),
237 area postrema (AP), and parabrachial nucleus (PBN), which are known to participate in
238 anorexigenic/satietogenic responses [40–43].
239 Chow- and HFD-fed mice were treated with JD-5037 (3 mg/kg, i.p.) or vehicle, and neuronal
240 activity was assessed in the NTS, AP, and PBN using cFos immunoreactivity as a *bonafide*
241 molecular proxy of neuronal activation. Strikingly, and in line with our earlier metabolic
242 observations (**Fig. 1, 2**), JD-5037 increased the number of cFos-positive cells in these brainstem
243 regions exclusively in HFD-fed mice (**Fig. 3A–D**). This suggests that peripheral CB1R
244 inhibition engages periphery-to-brain satiety circuits in a metabolic state-dependent manner.
245 Eating disorders and obesity are associated with a chronic elevation of circulating
246 endocannabinoids, particularly 2-arachidonoylglycerol (2-AG) and/or anandamide (AEA), in
247 both humans and animal models, reflecting a systemic overactivation of the endocannabinoid
248 system (ECS) [12,15,44–46]. Given the activation of the NTS observed in HFD-fed mice
249 following JD-5037 administration, we hypothesized that the vagus nerve, which conveys
250 peripheral metabolic/nutritional signals to NTS-neurons, undergoes CB1R-related molecular
251 adaptations. To explore this aspect, we first examined whether neurons in the nodose ganglia
252 (NG) express CB1R. Consistent with previous reports [9,32], transcriptomic meta-analysis
253 revealed a strong enrichment of *Cnr1* (the transcript encoding for CB1R) in *Phox2b*-positive
254 neurons of the NG (**Fig. 3E**). Furthermore, direct quantification of *Cnr1* expression in the NG
255 showed a significant upregulation in HFD-fed mice compared to chow-fed controls (**Fig. 3F**),
256 suggesting that obesity sensitizes vagal afferents to endocannabinoid signaling.
257 To directly assess whether JD-5037-induced cFos activation in the NTS/AP was mediated via
258 the gut-brain vagal axis, we employed the subdiaphragmatic vagotomy (SDV) model. In HFD-
259 fed mice that underwent SDV (SDV^{HFD}-mice), JD-5037 failed to elicit the robust cFos
260 activation observed in $Sham^{HFD}$-mice, with a dramatic reduction of cFos expression in the NTS,
261 AP and PBN (**Fig. 3G-J**). These findings indicate that peripheral CB1R inhibition activates
262 interconnected satiety-associated brainstem nuclei through a vagus nerve-dependent
263 mechanism.
264
265 **The gut-brain vagal axis is dispensable for the metabolic effects of peripheral CB1R**
266 **inhibition**

267 Although the gut-brain vagal axis is required for JD-5037-induced neuronal activation in the
268 brainstem, we next wondered whether this pathway was also necessary for the metabolic effects
269 of peripheral CB1R inhibition. To this end, we compared JD-5037-mediated metabolic
270 responses in Sham^{HFD}- *versus* SDV^{HFD}-mice by using calorimetric cages. In this experiment,
271 food was removed during the light phase (**Fig. 4A, B**; magenta area) to isolate metabolic
272 responses from food intake (**Fig. 4A, B**; green area).
273 During this fasting period, JD-5037 administration had no impact on respiratory exchange ratio
274 (RER), fatty acid oxidation (FAO), or energy expenditure in either group (**Fig. 4C-H**),
275 confirming that food intake is required to reveal the metabolic shift of nutrient partitioning and
276 utilization. When food was reintroduced prior to the dark phase (**Fig. 4A, B**; green area), JD-
277 5037 significantly reduced food intake in Sham^{HFD}-mice (**Fig. 4A, A^{1}**) but surprisingly also in
278 SDV^{HFD}-mice (**Fig. 4B, B^{1}**). In addition, JD-5037-induced changes in nutrient utilization,
279 characterized by a reduced RER and an enhanced FAO, were observed in both groups (**Fig. 4C-**
280 **F^{1}**), with no significant differences in energy expenditure (**Fig. 4G-H^{1}**). These results suggest
281 that, although the gut-brain vagal axis is essential for the central activation of satiety-associated
282 brainstem nuclei (**Fig. 3**), it is not required for the neither the metabolic effects nor the change
283 in food intake (FI) triggered by the inhibition of peripheral CB1R.
284 To further validate the dispensability of gut-brain vagal signaling in the metabolic effects of
285 peripheral CB1R inhibition, we pharmacologically blocked the action of two key gut-derived
286 hormones: cholecystokinin (CCK) and glucagon-like peptide-1 (GLP-1). These incretins are (*i*)
287 known to be regulated by CB1R [26,30,47,48] and (*ii*) well-established activators of vagal
288 afferents [49,50]. We co-administered the CCK receptor antagonist devazepide (**Fig. 5A**) or the
289 GLP-1 receptor antagonist exendin-(9-39) (**Fig. 5B**) along with JD-5037 in both chow- and
290 HFD-fed mice. Strikingly, neither antagonist reversed the anorexigenic effect of JD-5037 (**Fig.**
291 **5A, B**), indicating that blocking CCK or GLP-1 signaling does not impair the appetite-
292 suppressing action of peripheral CB1R inhibition. These findings further support the conclusion
293 that gut-brain endocrine signaling is not required for the metabolic benefits elicited by
294 peripherally acting CB1R antagonists in a HFD model.
295
296 **Inhibition of peripheral CB1R activates satietogenic hypothalamic nuclei in a metabolic**
297 **state-dependent but a vagus nerve-independent manner**
298 The hypothalamus is a central regulator of feeding behavior and energy homeostasis [51]. We
299 therefore examined whether peripheral CB1R inhibition triggered activation of two major
300 hypothalamic nuclei involved in appetite regulation: the paraventricular nucleus (PVN) and the

301 arcuate nucleus (ARC). JD-5037 significantly increased the number of cFos-positive cells in
302 both regions, but only in HFD-fed mice (**Fig. 6A-C**), reinforcing our earlier observations in the
303 brainstem (**Fig. 3**) that peripheral CB1R inhibition engages periphery-to-brain satiety pathways
304 in a metabolic state-dependent manner.
305 We next wondered whether this hypothalamic activation required an intact vagus nerve.
306 Unexpectedly, JD-5037 still induced robust activation of both the PVN- and ARC-neurons in
307 $Sham^{HFD}$- and SDV^{HFD}-mice (**Fig. 6D-F**).
308 Together, these findings indicate that peripheral CB1R inhibition activates interconnected
309 satiety-associated hypothalamic circuits through a vagus nerve-independent mechanism. This
310 mechanism, which differs from the one observed in the brainstem (**Fig. 3G-J**), may underlie
311 the comparable behavioral and metabolic improvements observed in $Sham^{HFD}$- and SDV^{HFD}-
312 mice (**Fig. 4**), pointing to a vagus-independent periphery-to-brain communication route driving
313 hypothalamic engagement.

314 **Discussion**

315 Our study provides compelling evidence that the metabolic efficacy of peripheral CB1 receptor
316 (CB1R) inhibition is strongly dependent on the metabolic state, with clear distinctions between
317 lean and diet-induced obese (DIO) mice. In fact, while peripherally restricted CB1R inverse
318 agonists such as JD-5037 had no measurable impact on feeding behavior, nutrient partitioning,
319 or energy expenditure in lean animals, the same treatment induced robust anorexigenic and
320 metabolic effects in HFD-fed mice. These findings underscore the importance of the metabolic
321 environment in modulating the responsiveness to peripheral endocannabinoid system (ECS)
322 manipulation and align to clinical and preclinical results indicating an exacerbated
323 endocannabinoid peripheral tone in different metabolic and eating disorders [3,6].

324 A key finding is also that inhibition of peripheral CB1R selectively reduced food intake and
325 shifted fuel utilization towards fatty acid oxidation in HFD-fed mice, consistent with previous
326 studies showing that ECS overactivation contributes to hyperphagia and metabolic dysfunctions
327 in obesity [3]. This metabolic state-dependence likely reflects (mal)adaptations in the ECS
328 peripheral tone, as evidenced by the upregulation of ECS-related signaling machinery and
329 CB1R in some peripheral organs [14,44,52,53] but also in the nodose ganglia of HFD-fed mice
330 (current study), a region that houses the sensory neurons of the vagus nerve and integrates
331 peripheral interoceptive/metabolic signals. This increase in vagal *Cnr1* may contribute, at least
332 in part, to the molecular and functional rearrangements underlying the blunted vagal activity
333 induced by chronic exposure to obesogenic diets [54–57].

334 Interestingly, we observed that peripheral CB1R inhibition activated satiety-associated
335 brainstem circuits, specifically the NTS, AP, and PBN, but only in HFD-fed animals. This
336 activation, visualized via increased cFos immunoreactivity and most likely resulting from a
337 CB1R-coupled Gi-dependent disinhibition, required an intact gut-brain vagal axis, as
338 subdiaphragmatic vagotomy strongly blunted JD-5037-induced cFos expression in the
339 brainstem. These data suggest that obesity-associated ECS overactivity sensitizes the gut-brain
340 vagal axis to peripheral CB1R blockade, thereby engaging central networks.

341 However, our findings also reveal a crucial dissociation: the gut-brain vagal axis is necessary
342 for neuronal activation in the brainstem but is dispensable for the metabolic effects of peripheral
343 CB1R inhibition. In fact, even in SDV^{HFD}-mice, JD-5037 retained its ability to reduce food
344 intake and shift nutrient partitioning, suggesting that peripheral mechanisms, independent of
345 gut-brain vagal inputs, are sufficient to mediate these homeostatic/metabolic outcomes. These
346 results, which are in line with a previous study showing that CB1R in vagal Phox2b-neurons is
347 dispensable for HFD-induced body weight gain [29], highlight that the vagal endocannabinoid

348 tone is mobilized in specific physio-pathological contexts such as binge eating [9], alcohol
349 preference/consumption [58,59], refeeding in fasted states [60] but not obesity, which is a
350 particular metabolic disorder. Furthermore, here we demonstrated that pharmacological
351 blockade of the gut hormones CCK and GLP-1, whose release and activity are scaled by CB1R-
352 related signaling [26,30,47,61], did not prevent the anorexigenic effects of JD-5037. This
353 finding further reinforces the notion that gut-derived endocrine signals are not critical mediators
354 of the metabolic effects elicited by peripheral CB1R antagonism. Thus, the persistence of JD-
355 5037 efficacy in the presence of CCK and GLP-1 antagonism suggests alternative, non-vagal
356 mechanisms that may be responsible for the metabolic improvements observed. These non-
357 vagal, CB1R-mediated body-brain mechanisms, may involve the release and/or clearance of
358 mediators from CB1R-expressing peripheral organs [13,27,62–65] in the bloodstream, the
359 involvement of the autonomic sympathetic nervous system [66,67] and/or the recruitment of
360 sensory spinal afferents [68,69], thereby modulating feeding and metabolic outputs
361 independently of gut-brain vagal inputs.
362 This interpretation is reinforced by our findings showing that the hypothalamic PVN and ARC
363 nuclei of obese mice, similar to brainstem nuclei, exhibit hypersensitivity to peripheral CB1R
364 inhibition, but through a mechanism independent of the vagus nerve. These results therefore
365 support the existence of alternative body-brain pathways capable of engaging hypothalamic
366 circuits without relying on the gut-brain vagal axis. Recently, it has been shown that JD-5037
367 restored leptin sensitivity in DIO mice [7,21], possibly by improving leptin transport across the
368 blood-brain barrier, thereby enabling hypothalamic action that may underlie the satietogenic
369 and metabolic effects induced by JD-5037.
370 An open question remains regarding the functional role of vagus-dependent brainstem circuits
371 activated (cFos induction) following peripheral CB1R inhibition. One plausible hypothesis is
372 that CB1R-mediated vagal signaling does not primarily influence homeostatic feeding and
373 peripheral energy metabolism, but instead modulates the hedonic, reward-driven aspects of
374 food intake [9,70]. Future studies should explore whether the reward deficits observed in obese
375 individuals may, at least in part, stem from dysfunctions in the gut-brain endocannabinoid vagal
376 system. This possibility is supported by evidence that pharmacological elevation of 2-AG levels
377 using the MAGL inhibitor JZL184 induces binge eating behavior in a vagus-dependent manner
378 [9].
379 Taken together, our results lead us to propose a dual-pathway model for the action of peripheral
380 CB1R antagonists in obesity: (*i*) a vagus-dependent neuronal activation of brainstem nuclei,
381 and (*ii*) a vagus-independent homeostatic/metabolic pathway, likely involving direct peripheral

effects on organs such as adipose tissue, liver, and/or the gastrointestinal tract which, in turn, may release endocrine mediators ultimately acting on the hypothalamus. This model reconciles the CNS effects of peripheral CB1R inhibition [9,71–73] with the sustained metabolic benefits seen in the absence of vagal or incretin signaling. Our findings have significant implications for the development of peripherally restricted CB1R antagonists as therapeutics for obesity and related metabolic disorders. The state-dependent responsiveness to peripheral CB1R blockade highlights the need to consider individual metabolic states when evaluating therapeutic efficacy. Moreover, the dissociation between neuronal activation and metabolic improvements suggests that engagement of satiety-associated brainstem circuits, while desirable, may not be required for metabolic benefits, potentially reducing the risk of CNS-mediated side effects.

Future work should focus on identifying the peripheral cellular targets of CB1R inhibition that mediate the observed shifts in energy balance and nutrient utilization. It will also be important to determine whether similar mechanisms operate in humans and whether biomarkers of ECS overactivity (*e.g.,* circulating endocannabinoid levels or CB1R expression profiles) can predict responsiveness to peripheral CB1R-based therapies.

Acknowledgments

We thank Olja Kacanski for administrative support; Isabelle Le Parco, Daniel Quintas, Magguy Boa, Ludovic Maingault, Angélique Dauvin and Florianne Michel for animals' care. We acknowledge the Functional and Physiological Exploration platform (FPE) of the Université Paris Cité, CNRS, *Unité de Biologie Fonctionnelle et Adaptative*, and the animal core facility "Buffon" of the Université Paris Cité/Institut Jacques Monod. We also thank Fabrice Licata of the BioMedTech Facilities (INSERM US36, CNRS UAR2009, Université Paris Cité) for help with data acquisition and technical advice.

Funding

This work was supported by the *Agence Nationale de la Recherche* (ANR-21-CE14-0021-01, ANR-23-CE14-0014-02, ANR-24-CE14-1322-03), *Fédération pour la Recherche sur le Cerveau*, *Institut universtaire de France* (IUF), *Plan d'investissement* France 2030 and Idex Emergence (ANR-18-IDEX-0001), IReSP (AAP-2023-SPA-13), Université Paris Cité and CNRS (to G.G.). O.O. is supported by a PhD fellowship from the *Fondation pour la Recherche Médicale* (FRM). G.G. was also partially supported by EMBO and the Alexander von Humboldt Foundation.

Author contributions

O.O. initiated and developed the project, performed and analyzed most of the experiments, critically contributed to the overall design and execution. C.d.A., B.B. and A.A. contributed to performing experiments. J.C. performed surgery. S.L. provided critical feedback. G.G. supervised the whole project, secured funding, provided guidance, designed the experimental plan, wrote and finalized the manuscript with the help of the co-authors.

Competing interests

The other authors declare no competing interests.

Data availability

All the data generated have been included in the article. Datasets are available from the corresponding author upon reasonable request.

References

[1] A. Furlan, P. Petrus, Brain-body communication in metabolic control, Trends Endocrinol Metab 34 (2023) 813–822. https://doi.org/10.1016/j.tem.2023.08.014.

[2] S. Saeed, A. Bonnefond, P. Froguel, Obesity: exploring its connection to brain function through genetic and genomic perspectives, Mol Psychiatry 30 (2025) 651–658. https://doi.org/10.1038/s41380-024-02737-9.

[3] W. Mazier, N. Saucisse, B. Gatta-Cherifi, D. Cota, The Endocannabinoid System: Pivotal Orchestrator of Obesity and Metabolic Disease, Trends Endocrinol Metab 26 (2015) 524–537. https://doi.org/10.1016/j.tem.2015.07.007.

[4] C. Quarta, R. Mazza, S. Obici, R. Pasquali, U. Pagotto, Energy balance regulation by endocannabinoids at central and peripheral levels, Trends Mol Med 17 (2011) 518–526. https://doi.org/10.1016/j.molmed.2011.05.002.

[5] B.K. Lau, D. Cota, L. Cristino, S.L. Borgland, Endocannabinoid modulation of homeostatic and non-homeostatic feeding circuits, Neuropharmacology 124 (2017) 38–51. https://doi.org/10.1016/j.neuropharm.2017.05.033.

[6] C. Quarta, D. Cota, Anti-obesity therapy with peripheral CB1 blockers: from promise to safe(?) practice, Int J Obes (Lond) 44 (2020) 2179–2193. https://doi.org/10.1038/s41366-020-0577-8.

[7] J. Tam, G. Szanda, A. Drori, Z. Liu, R. Cinar, Y. Kashiwaya, M.L. Reitman, G. Kunos, Peripheral cannabinoid-1 receptor blockade restores hypothalamic leptin signaling, Mol Metab 6 (2017) 1113–1125. https://doi.org/10.1016/j.molmet.2017.06.010.

[8] J. Tam, V.K. Vemuri, J. Liu, S. Bátkai, B. Mukhopadhyay, G. Godlewski, D. Osei-Hyiaman, S. Ohnuma, S.V. Ambudkar, J. Pickel, A. Makriyannis, G. Kunos, Peripheral CB1 cannabinoid receptor blockade improves cardiometabolic risk in mouse models of obesity, J Clin Invest 120 (2010) 2953–2966. https://doi.org/10.1172/JCI42551.

[9] C. Berland, J. Castel, R. Terrasi, E. Montalban, E. Foppen, C. Martin, G.G. Muccioli, S. Luquet, G. Gangarossa, Identification of an endocannabinoid gut-brain vagal mechanism controlling food reward and energy homeostasis, Mol Psychiatry 27 (2022) 2340–2354. https://doi.org/10.1038/s41380-021-01428-z.

[10] I. Knani, B.J. Earley, S. Udi, A. Nemirovski, R. Hadar, A. Gammal, R. Cinar, H.J. Hirsch, Y. Pollak, I. Gross, T. Eldar-Geva, D.P. Reyes-Capo, J.C. Han, A.M. Haqq, V. Gross-Tsur, R. Wevrick, J. Tam, Targeting the endocannabinoid/CB1 receptor system for treating obesity in Prader-Willi syndrome, Mol Metab 5 (2016) 1187–1199. https://doi.org/10.1016/j.molmet.2016.10.004.

[11] A.M. Monteleone, F. Piscitelli, R. Dalle Grave, M. El Ghoch, V. Di Marzo, M. Maj, P. Monteleone, Peripheral Endocannabinoid Responses to Hedonic Eating in Binge-Eating Disorder, Nutrients 9 (2017) 1377. https://doi.org/10.3390/nu9121377.

[12] P. Monteleone, I. Matias, V. Martiadis, L. De Petrocellis, M. Maj, V. Di Marzo, Blood levels of the endocannabinoid anandamide are increased in anorexia nervosa and in binge-eating disorder, but not in bulimia nervosa, Neuropsychopharmacology 30 (2005) 1216–1221. https://doi.org/10.1038/sj.npp.1300695.

[13] D.A. Argueta, N.V. DiPatrizio, Peripheral endocannabinoid signaling controls hyperphagia in western diet-induced obesity, Physiol Behav 171 (2017) 32–39. https://doi.org/10.1016/j.physbeh.2016.12.044.

[14] E.N. Kuipers, V. Kantae, B.C.E. Maarse, S.M. van den Berg, R. van Eenige, K.J. Nahon, A. Reifel-Miller, T. Coskun, M.P.J. de Winther, E. Lutgens, S. Kooijman, A.C. Harms, T. Hankemeier, M. van der Stelt, P.C.N. Rensen, M.R. Boon, High Fat Diet Increases Circulating Endocannabinoids Accompanied by Increased Synthesis Enzymes in Adipose Tissue, Front Physiol 9 (2018) 1913. https://doi.org/10.3389/fphys.2018.01913.

[15] T.J. Little, N. Cvijanovic, N.V. DiPatrizio, D.A. Argueta, C.K. Rayner, C. Feinle-Bisset, R.L. Young, Plasma endocannabinoid levels in lean, overweight, and obese humans: relationships to intestinal permeability markers, inflammation, and incretin secretion, Am J Physiol Endocrinol Metab 315 (2018) E489–E495. https://doi.org/10.1152/ajpendo.00355.2017.

[16] V. Di Marzo, CB(1) receptor antagonism: biological basis for metabolic effects, Drug Discov Today 13 (2008) 1026–1041. https://doi.org/10.1016/j.drudis.2008.09.001.

[17] C.E. Beyer, J.M. Dwyer, M.J. Piesla, B.J. Platt, R. Shen, Z. Rahman, K. Chan, M.T. Manners, T.A. Samad, J.D. Kennedy, B. Bingham, G.T. Whiteside, Depression-like phenotype following chronic CB1 receptor antagonism, Neurobiol Dis 39 (2010) 148–155. https://doi.org/10.1016/j.nbd.2010.03.020.

[18] D.R. Janero, A. Makriyannis, Cannabinoid receptor antagonists: pharmacological opportunities, clinical experience, and translational prognosis, Expert Opin Emerg Drugs 14 (2009) 43–65. https://doi.org/10.1517/14728210902736568.

[19] B. Le Foll, A. Pushparaj, Y. Pryslawsky, B. Forget, K. Vemuri, A. Makriyannis, J.M. Trigo, Translational strategies for therapeutic development in nicotine addiction: rethinking the conventional bench to bedside approach, Prog Neuropsychopharmacol Biol Psychiatry 52 (2014) 86–93. https://doi.org/10.1016/j.pnpbp.2013.10.009.

[20] N.L. Cluny, V.K. Vemuri, A.P. Chambers, C.L. Limebeer, H. Bedard, J.T. Wood, B. Lutz, A. Zimmer, L.A. Parker, A. Makriyannis, K.A. Sharkey, A novel peripherally restricted cannabinoid receptor antagonist, AM6545, reduces food intake and body weight, but does not cause malaise, in rodents, Br J Pharmacol 161 (2010) 629–642. https://doi.org/10.1111/j.1476-5381.2010.00908.x.

[21] J. Tam, R. Cinar, J. Liu, G. Godlewski, D. Wesley, T. Jourdan, G. Szanda, B. Mukhopadhyay, L. Chedester, J.-S. Liow, R.B. Innis, K. Cheng, K.C. Rice, J.R. Deschamps, R.J. Chorvat, J.F. McElroy, G. Kunos, Peripheral cannabinoid-1 receptor inverse agonism reduces obesity by reversing leptin resistance, Cell Metab 16 (2012) 167–179. https://doi.org/10.1016/j.cmet.2012.07.002.

[22] J. Liu, G. Godlewski, T. Jourdan, Z. Liu, R. Cinar, K. Xiong, G. Kunos, Cannabinoid-1 Receptor Antagonism Improves Glycemic Control and Increases Energy Expenditure Through Sirtuin-1/Mechanistic Target of Rapamycin Complex 2 and 5'Adenosine Monophosphate-Activated Protein Kinase Signaling, Hepatology 69 (2019) 1535–1548. https://doi.org/10.1002/hep.30364.

[23] C. Roger, C. Buch, T. Muller, J. Leemput, L. Demizieux, P. Passilly-Degrace, R. Cinar, M.R. Iyer, G. Kunos, B. Vergès, P. Degrace, T. Jourdan, Simultaneous Inhibition of Peripheral CB1R and iNOS Mitigates Obesity-Related Dyslipidemia Through Distinct Mechanisms, Diabetes 69 (2020) 2120–2132. https://doi.org/10.2337/db20-0078.

[24] S. Tan, H. Liu, B. Ke, J. Jiang, B. Wu, The peripheral CB1 receptor antagonist JD5037 attenuates liver fibrosis via a CB1 receptor/β-arrestin1/Akt pathway, Br J Pharmacol 177 (2020) 2830–2847. https://doi.org/10.1111/bph.15010.

[25] L. Maccioni, S. Dvorácskó, G. Godlewski, R. Cinar, M.R. Iyer, B. Gao, G. Kunos, Gut cannabinoid receptor 1 regulates alcohol binge-induced intestinal permeability, eGastroenterology 3 (2025) e100173. https://doi.org/10.1136/egastro-2024-100173.

[26] P.A. Perez, M.B. Wiley, A. Makriyannis, N.V. DiPatrizio, Cannabinoids Block Fat-induced Incretin Release via CB1-dependent and CB1-independent Pathways in Intestinal Epithelium, Gastro Hep Adv 3 (2024) 931–941. https://doi.org/10.1016/j.gastha.2024.07.006.

[27] I. Ruiz de Azua, G. Mancini, R.K. Srivastava, A.A. Rey, P. Cardinal, L. Tedesco, C.M. Zingaretti, A. Sassmann, C. Quarta, C. Schwitter, A. Conrad, N. Wettschureck, V.K. Vemuri, A. Makriyannis, J. Hartwig, M. Mendez-Lago, L. Bindila, K. Monory, A.

Giordano, S. Cinti, G. Marsicano, S. Offermanns, E. Nisoli, U. Pagotto, D. Cota, B. Lutz, Adipocyte cannabinoid receptor CB1 regulates energy homeostasis and alternatively activated macrophages, J Clin Invest 127 (2017) 4148–4162. https://doi.org/10.1172/JCI83626.

[28] S. Wang, Q. Zhu, G. Liang, T. Franks, M. Boucher, K.K. Bence, M. Lu, C.M. Castorena, S. Zhao, J.K. Elmquist, P.E. Scherer, J.D. Horton, Cannabinoid receptor 1 signaling in hepatocytes and stellate cells does not contribute to NAFLD, J Clin Invest 131 (2021) e152242. https://doi.org/10.1172/JCI152242.

[29] C.R. Vianna, J. Donato, J. Rossi, M. Scott, K. Economides, L. Gautron, S. Pierpont, C.F. Elias, J.K. Elmquist, Cannabinoid receptor 1 in the vagus nerve is dispensable for body weight homeostasis but required for normal gastrointestinal motility, J Neurosci 32 (2012) 10331–10337. https://doi.org/10.1523/JNEUROSCI.4507-11.2012.

[30] D.A. Argueta, P.A. Perez, A. Makriyannis, N.V. DiPatrizio, Cannabinoid CB1 Receptors Inhibit Gut-Brain Satiation Signaling in Diet-Induced Obesity, Front Physiol 10 (2019) 704. https://doi.org/10.3389/fphys.2019.00704.

[31] A.G. Sykaras, C. Demenis, R.M. Case, J.T. McLaughlin, C.P. Smith, Duodenal enteroendocrine I-cells contain mRNA transcripts encoding key endocannabinoid and fatty acid receptors, PLoS One 7 (2012) e42373. https://doi.org/10.1371/journal.pone.0042373.

[32] K.L. Egerod, N. Petersen, P.N. Timshel, J.C. Rekling, Y. Wang, Q. Liu, T.W. Schwartz, L. Gautron, Profiling of G protein-coupled receptors in vagal afferents reveals novel gut-to-brain sensing mechanisms, Mol Metab 12 (2018) 62–75. https://doi.org/10.1016/j.molmet.2018.03.016.

[33] G. Burdyga, S. Lal, A. Varro, R. Dimaline, D.G. Thompson, G.J. Dockray, Expression of cannabinoid CB1 receptors by vagal afferent neurons is inhibited by cholecystokinin, J Neurosci 24 (2004) 2708–2715. https://doi.org/10.1523/JNEUROSCI.5404-03.2004.

[34] O. Onimus, F. Arrivet, I.N. de O. Souza, B. Bertrand, J. Castel, S. Luquet, J.-P. Mothet, N. Heck, G. Gangarossa, The gut-brain vagal axis scales hippocampal memory processes and plasticity, Neurobiol Dis 199 (2024) 106569. https://doi.org/10.1016/j.nbd.2024.106569.

[35] G. Gangarossa, L. Castell, L. Castro, P. Tarot, F. Veyrunes, P. Vincent, F. Bertaso, E. Valjent, Contrasting patterns of ERK activation in the tail of the striatum in response to aversive and rewarding signals, J Neurochem 151 (2019) 204–226. https://doi.org/10.1111/jnc.14804.

[36] O. Onimus, E. Valjent, G. Fisone, G. Gangarossa, Haloperidol-Induced Immediate Early Genes in Striatopallidal Neurons Requires the Converging Action of cAMP/PKA/DARPP-32 and mTOR Pathways, Int J Mol Sci 23 (2022) 11637. https://doi.org/10.3390/ijms231911637.

[37] J. Castel, G. Li, O. Onimus, E. Leishman, P.D. Cani, H. Bradshaw, K. Mackie, A. Everard, S. Luquet, G. Gangarossa, NAPE-PLD in the ventral tegmental area regulates reward events, feeding and energy homeostasis, Mol Psychiatry 29 (2024) 1478–1490. https://doi.org/10.1038/s41380-024-02427-6.

[38] L. Bai, S. Mesgarzadeh, K.S. Ramesh, E.L. Huey, Y. Liu, L.A. Gray, T.J. Aitken, Y. Chen, L.R. Beutler, J.S. Ahn, L. Madisen, H. Zeng, M.A. Krasnow, Z.A. Knight, Genetic Identification of Vagal Sensory Neurons That Control Feeding, Cell 179 (2019) 1129-1143.e23. https://doi.org/10.1016/j.cell.2019.10.031.

[39] J. Tam, L. Hinden, A. Drori, S. Udi, S. Azar, S. Baraghithy, The therapeutic potential of targeting the peripheral endocannabinoid/CB1 receptor system, Eur J Intern Med 49 (2018) 23–29. https://doi.org/10.1016/j.ejim.2018.01.009.

[40] I.C. Alcantara, A.P.M. Tapia, Y. Aponte, M.J. Krashes, Acts of appetite: neural circuits governing the appetitive, consummatory, and terminating phases of feeding, Nat Metab 4 (2022) 836–847. https://doi.org/10.1038/s42255-022-00611-y.
[41] G. D'Agostino, D. Lyons, C. Cristiano, M. Lettieri, C. Olarte-Sanchez, L.K. Burke, M. Greenwald-Yarnell, C. Cansell, B. Doslikova, T. Georgescu, P.B. Martinez de Morentin, M.G. Myers, J.J. Rochford, L.K. Heisler, Nucleus of the Solitary Tract Serotonin 5-HT2C Receptors Modulate Food Intake, Cell Metab 28 (2018) 619-630.e5. https://doi.org/10.1016/j.cmet.2018.07.017.
[42] M.R. Hayes, K.P. Skibicka, T.M. Leichner, D.J. Guarnieri, R.J. DiLeone, K.K. Bence, H.J. Grill, Endogenous leptin signaling in the caudal nucleus tractus solitarius and area postrema is required for energy balance regulation, Cell Metab 11 (2010) 77–83. https://doi.org/10.1016/j.cmet.2009.10.009.
[43] C.W. Roman, V.A. Derkach, R.D. Palmiter, Genetically and functionally defined NTS to PBN brain circuits mediating anorexia, Nat Commun 7 (2016) 11905. https://doi.org/10.1038/ncomms11905.
[44] S. Engeli, J. Böhnke, M. Feldpausch, K. Gorzelniak, J. Janke, S. Bátkai, P. Pacher, J. Harvey-White, F.C. Luft, A.M. Sharma, J. Jordan, Activation of the peripheral endocannabinoid system in human obesity, Diabetes 54 (2005) 2838–2843. https://doi.org/10.2337/diabetes.54.10.2838.
[45] I. Matias, B. Gatta-Cherifi, A. Tabarin, S. Clark, T. Leste-Lasserre, G. Marsicano, P.V. Piazza, D. Cota, Endocannabinoids measurement in human saliva as potential biomarker of obesity, PLoS One 7 (2012) e42399. https://doi.org/10.1371/journal.pone.0042399.
[46] N. Mattelaer, B. Van der Schueren, L. Van Oudenhove, N. Weltens, R. Vangoitsenhoven, The circulating and central endocannabinoid system in obesity and weight loss, Int J Obes (Lond) 48 (2024) 1363–1382. https://doi.org/10.1038/s41366-024-01553-z.
[47] I. González-Mariscal, S.M. Krzysik-Walker, W. Kim, M. Rouse, J.M. Egan, Blockade of cannabinoid 1 receptor improves GLP-1R mediated insulin secretion in mice, Mol Cell Endocrinol 423 (2016) 1–10. https://doi.org/10.1016/j.mce.2015.12.015.
[48] C.E. Moss, W.J. Marsh, H.E. Parker, E. Ogunnowo-Bada, C.H. Riches, A.M. Habib, M.L. Evans, F.M. Gribble, F. Reimann, Somatostatin receptor 5 and cannabinoid receptor 1 activation inhibit secretion of glucose-dependent insulinotropic polypeptide from intestinal K cells in rodents, Diabetologia 55 (2012) 3094–3103. https://doi.org/10.1007/s00125-012-2663-5.
[49] H.-R. Berthoud, V.L. Albaugh, W.L. Neuhuber, Gut-brain communication and obesity: understanding functions of the vagus nerve, J Clin Invest 131 (2021) e143770, 143770. https://doi.org/10.1172/JCI143770.
[50] C. Clemmensen, T.D. Müller, S.C. Woods, H.-R. Berthoud, R.J. Seeley, M.H. Tschöp, Gut-Brain Cross-Talk in Metabolic Control, Cell 168 (2017) 758–774. https://doi.org/10.1016/j.cell.2017.01.025.
[51] J.C. Brüning, H. Fenselau, Integrative neurocircuits that control metabolism and food intake, Science 381 (2023) eabl7398. https://doi.org/10.1126/science.abl7398.
[52] M. Côté, I. Matias, I. Lemieux, S. Petrosino, N. Alméras, J.-P. Després, V. Di Marzo, Circulating endocannabinoid levels, abdominal adiposity and related cardiometabolic risk factors in obese men, Int J Obes (Lond) 31 (2007) 692–699. https://doi.org/10.1038/sj.ijo.0803539.
[53] I. Matias, S. Petrosino, A. Racioppi, R. Capasso, A.A. Izzo, V. Di Marzo, Dysregulation of peripheral endocannabinoid levels in hyperglycemia and obesity: Effect of high fat diets, Mol Cell Endocrinol 286 (2008) S66-78. https://doi.org/10.1016/j.mce.2008.01.026.

[54] D.M. Daly, S.J. Park, W.C. Valinsky, M.J. Beyak, Impaired intestinal afferent nerve satiety signalling and vagal afferent excitability in diet induced obesity in the mouse, J Physiol 589 (2011) 2857–2870. https://doi.org/10.1113/jphysiol.2010.204594.

[55] G. de Lartigue, Role of the vagus nerve in the development and treatment of diet-induced obesity, J Physiol 594 (2016) 5791–5815. https://doi.org/10.1113/JP271538.

[56] G. de Lartigue, C. Barbier de la Serre, E. Espero, J. Lee, H.E. Raybould, Diet-induced obesity leads to the development of leptin resistance in vagal afferent neurons, Am J Physiol Endocrinol Metab 301 (2011) E187-195. https://doi.org/10.1152/ajpendo.00056.2011.

[57] H. Loper, M. Leinen, L. Bassoff, J. Sample, M. Romero-Ortega, K.J. Gustafson, D.M. Taylor, M.A. Schiefer, Both high fat and high carbohydrate diets impair vagus nerve signaling of satiety, Sci Rep 11 (2021) 10394. https://doi.org/10.1038/s41598-021-89465-0.

[58] G. Godlewski, R. Cinar, N.J. Coffey, J. Liu, T. Jourdan, B. Mukhopadhyay, L. Chedester, Z. Liu, D. Osei-Hyiaman, M.R. Iyer, J.K. Park, R.G. Smith, H. Iwakura, G. Kunos, Targeting Peripheral CB1 Receptors Reduces Ethanol Intake via a Gut-Brain Axis, Cell Metab 29 (2019) 1320-1333.e8. https://doi.org/10.1016/j.cmet.2019.04.012.

[59] A. Herrerias, A. Oliverio, S. Dvorácskó, A. Thyagarajan, L. Chedester, J. Liu, R. Cinar, M.R. Iyer, G. Kunos, G. Godlewski, CB1 receptors on a subset of vagal afferent neurons modulate voluntary ethanol intake in mice, Mol Psychiatry (2025). https://doi.org/10.1038/s41380-025-03266-9.

[60] R. Gómez, M. Navarro, B. Ferrer, J.M. Trigo, A. Bilbao, I. Del Arco, A. Cippitelli, F. Nava, D. Piomelli, F. Rodríguez de Fonseca, A peripheral mechanism for CB1 cannabinoid receptor-dependent modulation of feeding, J Neurosci 22 (2002) 9612–9617. https://doi.org/10.1523/JNEUROSCI.22-21-09612.2002.

[61] C.P. Wood, C. Alvarez, N.V. DiPatrizio, Cholinergic Neurotransmission Controls Orexigenic Endocannabinoid Signaling in the Gut in Diet-Induced Obesity, J Neurosci 44 (2024) e0813232024. https://doi.org/10.1523/JNEUROSCI.0813-23.2024.

[62] N.P. Bowles, I.N. Karatsoreos, X. Li, V.K. Vemuri, J.-A. Wood, Z. Li, K.L.K. Tamashiro, G.J. Schwartz, A.M. Makriyannis, G. Kunos, C.J. Hillard, B.S. McEwen, M.N. Hill, A peripheral endocannabinoid mechanism contributes to glucocorticoid-mediated metabolic syndrome, Proc Natl Acad Sci U S A 112 (2015) 285–290. https://doi.org/10.1073/pnas.1421420112.

[63] A. Drori, A. Gammal, S. Azar, L. Hinden, R. Hadar, D. Wesley, A. Nemirovski, G. Szanda, M. Salton, B. Tirosh, J. Tam, CB1R regulates soluble leptin receptor levels via CHOP, contributing to hepatic leptin resistance, Elife 9 (2020) e60771. https://doi.org/10.7554/eLife.60771.

[64] A. Ghosh, M.-L. Peyot, Y.H. Leung, F. Ravenelle, S.R.M. Madiraju, M. Prentki, A peripherally restricted cannabinoid-1 receptor inverse agonist promotes insulin secretion and protects from cytokine toxicity in human pancreatic islets, Eur J Pharmacol 944 (2023) 175589. https://doi.org/10.1016/j.ejphar.2023.175589.

[65] T. Jourdan, J.K. Park, Z.V. Varga, J. Pálóczi, N.J. Coffey, A.Z. Rosenberg, G. Godlewski, R. Cinar, K. Mackie, P. Pacher, G. Kunos, Cannabinoid-1 receptor deletion in podocytes mitigates both glomerular and tubular dysfunction in a mouse model of diabetic nephropathy, Diabetes Obes Metab 20 (2018) 698–708. https://doi.org/10.1111/dom.13150.

[66] L. Bellocchio, E. Soria-Gómez, C. Quarta, M. Metna-Laurent, P. Cardinal, E. Binder, A. Cannich, A. Delamarre, M. Häring, M. Martín-Fontecha, D. Vega, T. Leste-Lasserre, D. Bartsch, K. Monory, B. Lutz, F. Chaouloff, U. Pagotto, M. Guzman, D. Cota, G. Marsicano, Activation of the sympathetic nervous system mediates hypophagic and

anxiety-like effects of CB_1 receptor blockade, Proc Natl Acad Sci U S A 110 (2013) 4786–4791. https://doi.org/10.1073/pnas.1218573110.

[67] C. Quarta, L. Bellocchio, G. Mancini, R. Mazza, C. Cervino, L.J. Braulke, C. Fekete, R. Latorre, C. Nanni, M. Bucci, L.E. Clemens, G. Heldmaier, M. Watanabe, T. Leste-Lassere, M. Maitre, L. Tedesco, F. Fanelli, S. Reuss, S. Klaus, R.K. Srivastava, K. Monory, A. Valerio, A. Grandis, R. De Giorgio, R. Pasquali, E. Nisoli, D. Cota, B. Lutz, G. Marsicano, U. Pagotto, CB(1) signaling in forebrain and sympathetic neurons is a key determinant of endocannabinoid actions on energy balance, Cell Metab 11 (2010) 273–285. https://doi.org/10.1016/j.cmet.2010.02.015.

[68] H. Münzberg, H.-R. Berthoud, W.L. Neuhuber, Sensory spinal interoceptive pathways and energy balance regulation, Molecular Metabolism 78 (2023) 101817. https://doi.org/10.1016/j.molmet.2023.101817.

[69] G. Veress, Z. Meszar, D. Muszil, A. Avelino, K. Matesz, K. Mackie, I. Nagy, Characterisation of cannabinoid 1 receptor expression in the perikarya, and peripheral and spinal processes of primary sensory neurons, Brain Struct Funct 218 (2013) 733–750. https://doi.org/10.1007/s00429-012-0425-2.

[70] W. Han, L.A. Tellez, M.H. Perkins, I.O. Perez, T. Qu, J. Ferreira, T.L. Ferreira, D. Quinn, Z.-W. Liu, X.-B. Gao, M.M. Kaelberer, D.V. Bohórquez, S.J. Shammah-Lagnado, G. de Lartigue, I.E. de Araujo, A Neural Circuit for Gut-Induced Reward, Cell 175 (2018) 665-678.e23. https://doi.org/10.1016/j.cell.2018.08.049.

[71] A. Bergadà-Martínez, L. de Los Reyes-Ramírez, S. Martínez-Torres, L. Ciaran-Alfano, I. Martínez-Gallego, R. Maldonado, A. Rodríguez-Moreno, A. Ozaita, Sub-chronic administration of AM6545 enhances cognitive performance and induces hippocampal synaptic plasticity changes in naïve mice, Br J Pharmacol (2025). https://doi.org/10.1111/bph.70015.

[72] A. Busquets-Garcia, M. Gomis-González, R.K. Srivastava, L. Cutando, A. Ortega-Alvaro, S. Ruehle, F. Remmers, L. Bindila, L. Bellocchio, G. Marsicano, B. Lutz, R. Maldonado, A. Ozaita, Peripheral and central CB1 cannabinoid receptors control stress-induced impairment of memory consolidation, Proc Natl Acad Sci U S A 113 (2016) 9904–9909. https://doi.org/10.1073/pnas.1525066113.

[73] S. Martínez-Torres, A. Bergadà-Martínez, J.E. Ortega, L. Galera-López, A. Hervera, L. de Los Reyes-Ramírez, A. Ortega-Álvaro, F. Remmers, E. Muñoz-Moreno, G. Soria, J.A. Del Río, B. Lutz, J.Á. Ruíz-Ortega, J.J. Meana, R. Maldonado, A. Ozaita, Peripheral CB1 receptor blockade acts as a memory enhancer through a noradrenergic mechanism, Neuropsychopharmacology 48 (2023) 341–350. https://doi.org/10.1038/s41386-022-01436-9.

711 **Figures and Figure legends**

Figure 1

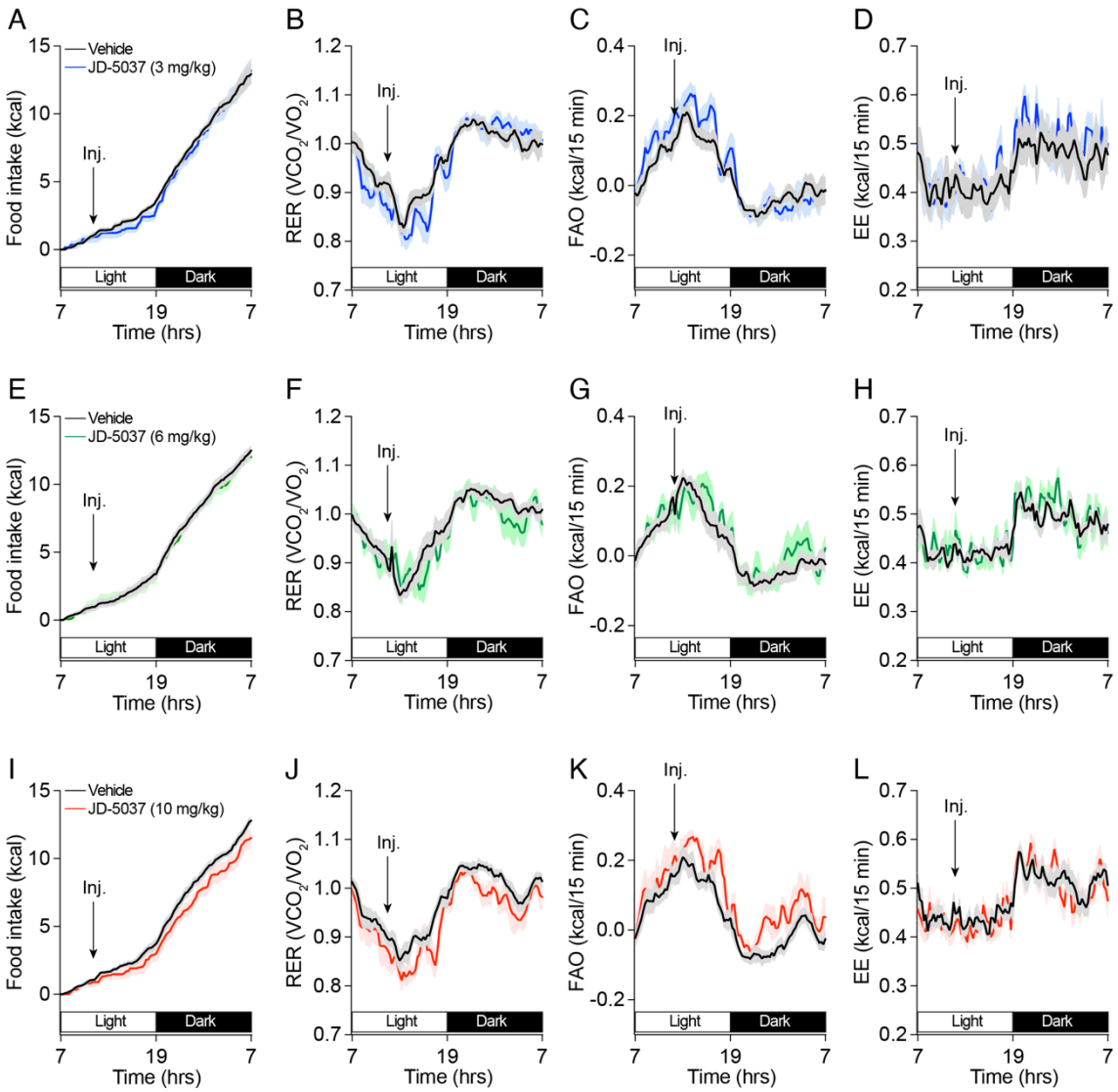

712

713 **Figure 1: Inhibition of peripheral CB1R does not affect feeding and energy homeostasis**
714 **in lean mice.** Escalating doses (3, 6, 10 mg/kg) of the peripheral CB1R inverse agonist JD-
715 5037 were administered to lean mice, and their feeding and metabolic profiles were
716 characterized by using metabolic chambers (indirect calorimetry). (**A, E, I**) Food intake, (**B, F,**
717 **J**) respiratory exchange ratio (RER), (**C, G, K**) fatty acid oxidation (FAO) and (**D, H, L**) energy
718 expenditure (EE) in mice injected with vehicle or JD-5037 (3, 6, 10 mg/kg) (n=6-7 mice/group).
719 Statistics: Two-way ANOVA followed by a Bonferroni *post hoc* test (all panels), not significant.

Figure 2

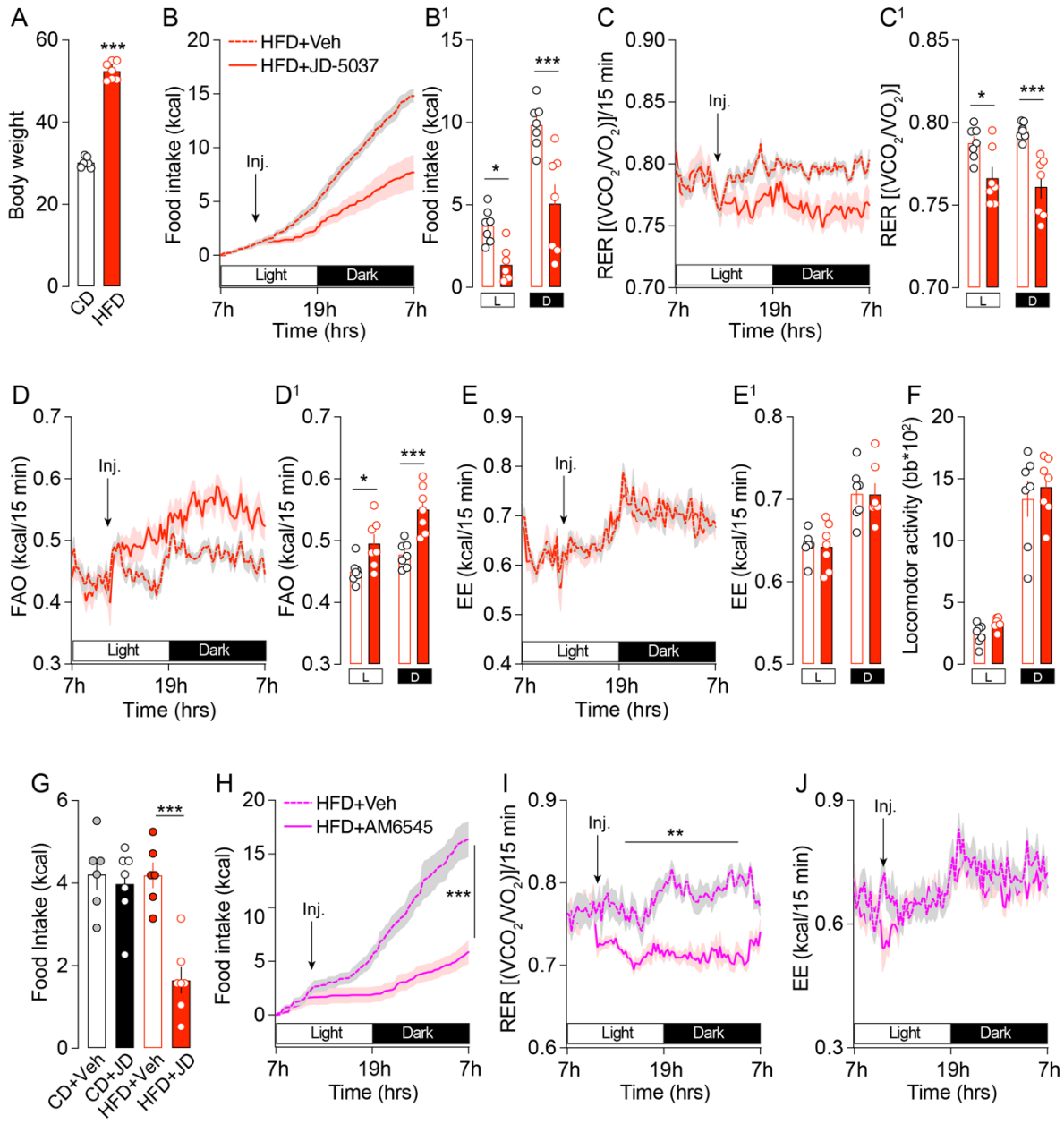

Figure 2: Inhibition of peripheral CB1R affects feeding and nutrient partitioning in HFD-mice. (**A**) HFD-induced body weight gain. Veh or JD-5037 (3 mg/kg) were administered to HFD-mice and their feeding and metabolic profiles were characterized by using metabolic chambers (indirect calorimetry). (**B, B^1**) Food intake, (**C, C^1**) respiratory exchange ratio (RER), (**D, D^1**) fatty acid oxidation (FAO), (**E, E^1**) energy expenditure (EE) and (**F**) spontaneous locomotor activity in HFD-mice injected with vehicle or JD-5037 (3 mg/kg) (n=7 mice/group). (**G**) Food intake in fasted chow diet- and HFD-mice 4 hours after refeeding schedule (n=6-7 mice/group). (**H**) Food intake, (**I**) RER and (**J**) EE in HFD-mice injected with vehicle or the

729 peripheral CB1R neutral antagonist AM6545 (3 mg/kg) (n=7 mice/group). Statistics: Student's
730 t-test (A panel), Two-way ANOVA followed by a Bonferroni *post hoc* test (B^1, C^1, D^1, E^1, F, H,
731 I, J panels), One-ways ANOVA followed by a Bonferroni *post hoc* test (G panel), *$p<0.05$,
732 **$p<0.01$ and ***$p<0.001$ for specific comparisons.

Figure 3

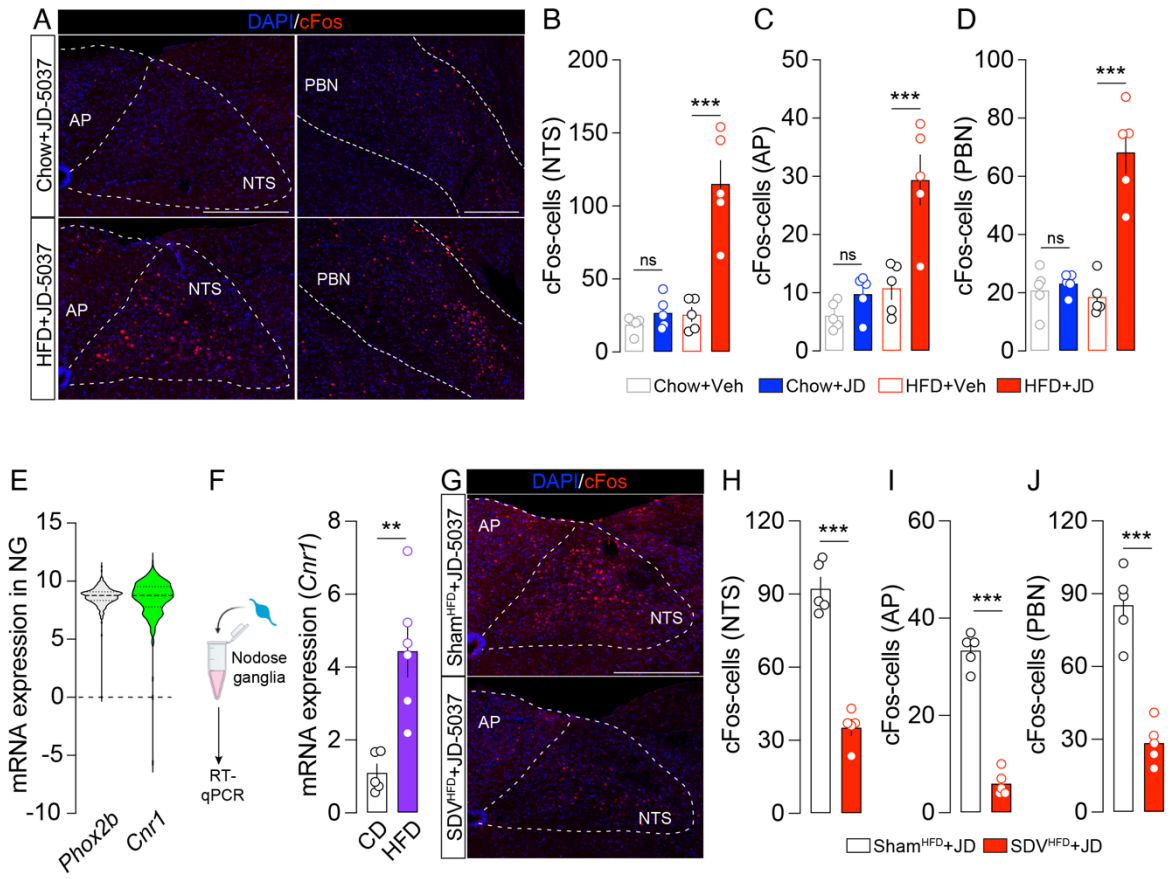

Figure 3: Inhibition of peripheral CB1R leads to the activation of brainstem nuclei via a vagus nerve-dependent mechanism. (**A**) Immunofluorescence detection of cFos in the nucleus tractus solitarius (NTS), area postrema (AP), and parabrachial nucleus (PBN) of chow- and HFD-mice administered with JD-5037 (3 mg/kg). Quantifications of cFos-positive cells in the NTS (**B**), AP (**C**) and PBN (**D**) of chow- and HFD-mice administered with vehicle or JD-5037 (3 mg/kg) (n=5 mice/group). (**E**) Transcriptomic meta-analysis of *Phox2b* and *Cnr1* in sensory neurons (n=275) of the nodose ganglia (NG). (**F**) Relative mRNA expression of *Cnr1* in the nodose ganglia of chow- and HFD-mice (n=5-6 mice/group). (**G**) Immunofluorescence detection and quantifications (**H, I, J**) of cFos-positive cells in the NTS, AP and PBN of Sham^{HFD}- and SDV^{HFD}-mice administered with JD-5037 (3 mg/kg) (n=5 mice/group). Scale bars: 250 µm. Statistics: One-way ANOVA followed by a Bonferroni *post hoc* test (B, C, D panels) or Student's t-test (F, H, I, J panels), **p<0.01 and ***p<0.001 for specific comparisons.

Figure 4

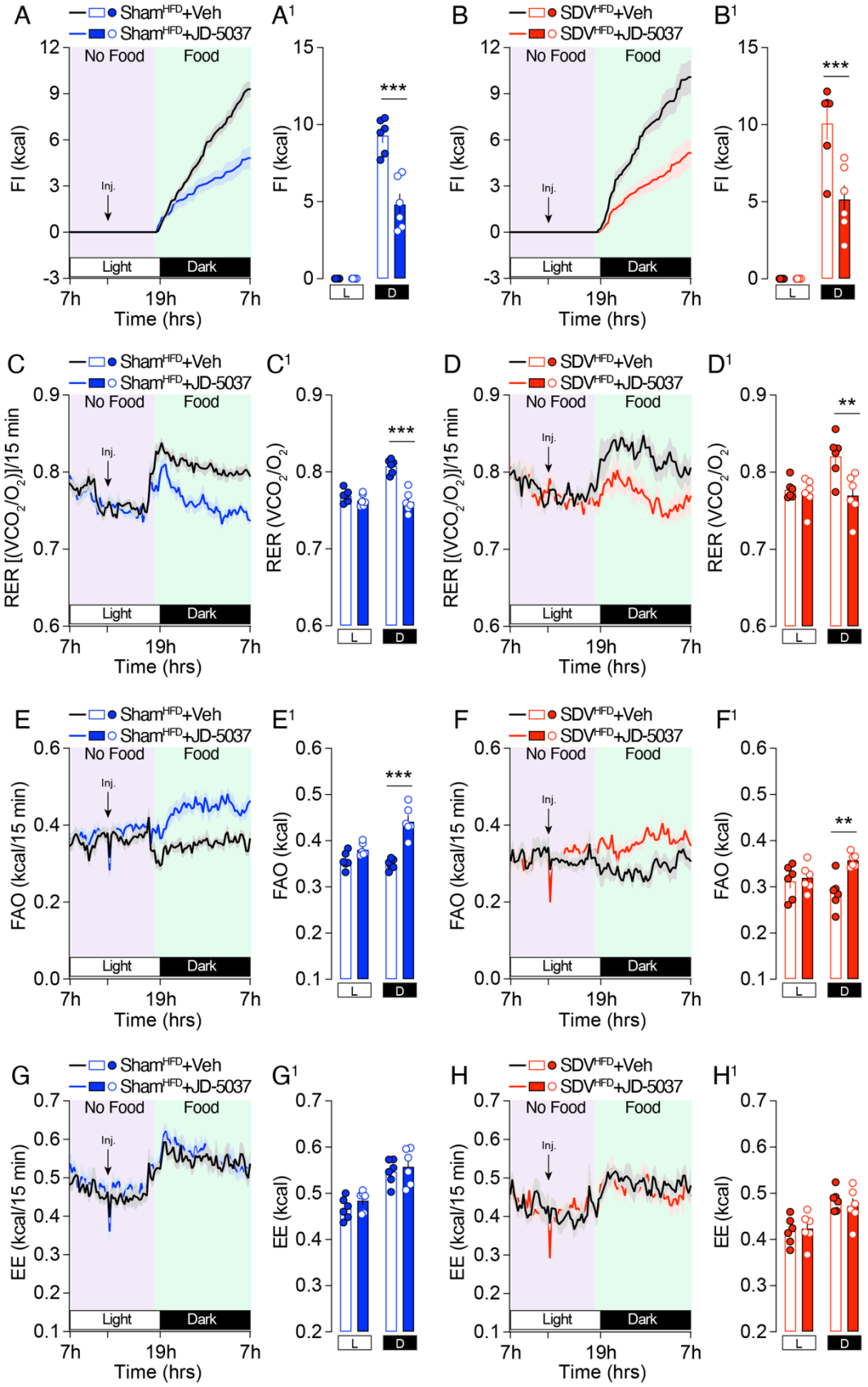
A
Sham^HFD+Veh
Sham^HFD+JD-5037
No Food
Food
Inj.
Light
Dark
FI (kcal)
Time (hrs)
7h
19h
7h
A1
***
L
D
B
SDV^HFD+Veh
SDV^HFD+JD-5037
B1
C
RER [(VCO2/O2)]/15 min
C1
RER (VCO2/O2)
D
D1
**
E
FAO (kcal/15 min)
E1
FAO (kcal)
F
F1
G
EE (kcal/15 min)
G1
EE (kcal)
H
H1

747

748 **Figure 4: The gut-brain vagal axis does not mediate JD-5037-induced feeding and**
749 **metabolic adaptations.** Veh or JD-5037 (3 mg/kg) were administered to $Sham^{HFD}$- and
750 SDV^{HFD}-mice and their feeding and metabolic profiles were characterized by using metabolic
751 chambers (indirect calorimetry). (**A, A^1, B, B^1**) Food intake, (**C, C^1, D, D^1**) respiratory exchange
752 ratio (RER), (**E, E^1, F, F^1**) fatty acid oxidation (FAO) and (**G, G^1, H, H^1**) energy expenditure
753 in $Sham^{HFD}$- and SDV^{HFD}-mice injected with vehicle or JD-5037 (3 mg/kg) (n=6 mice/group).
754 Statistics: Two-way ANOVA followed by a Bonferroni *post hoc* test (all panels), **$p<0.01$ and
755 ***$p<0.001$ for specific comparisons.

Figure 5

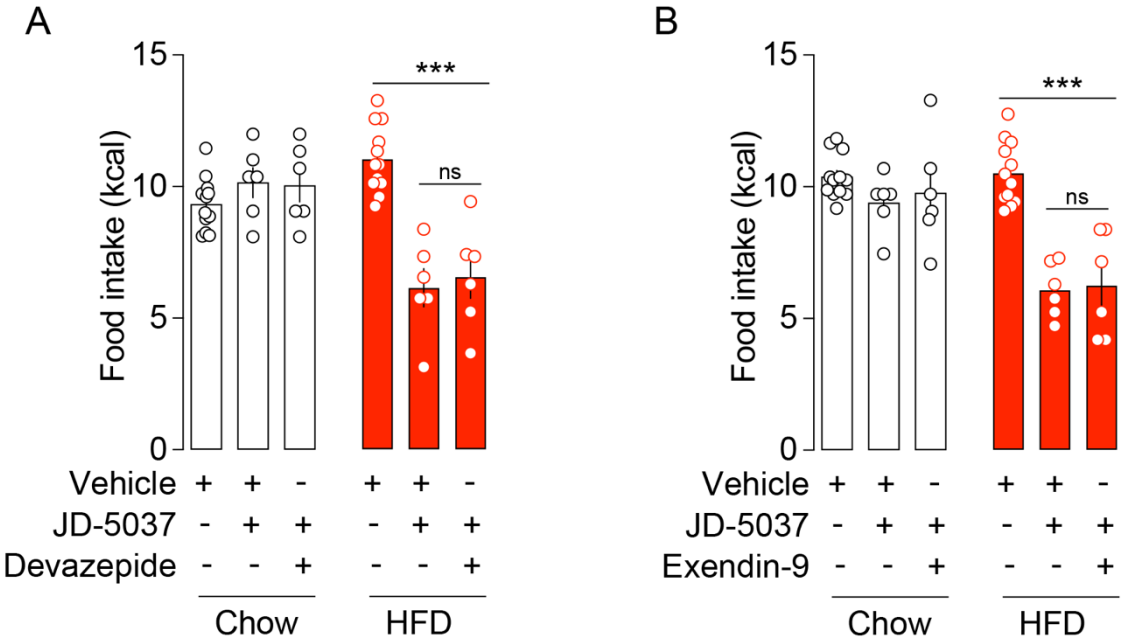

Figure 5: CCK and GLP-1 do not mediate JD-5037-induced feeding adaptations. (**A, B**) Food intake in lean and HFD-mice following administration the CCK receptor antagonist devazepide (0.3 mg/kg) (**A**) or the GLP1 receptor antagonist Exendin-9 (0.1 mg/kg) (**B**) (n=6-12 mice/group). Statistics: Two-way ANOVA followed by a Bonferroni *post hoc* test (all panels), ***p<0.001 for specific comparisons.

Figure 6

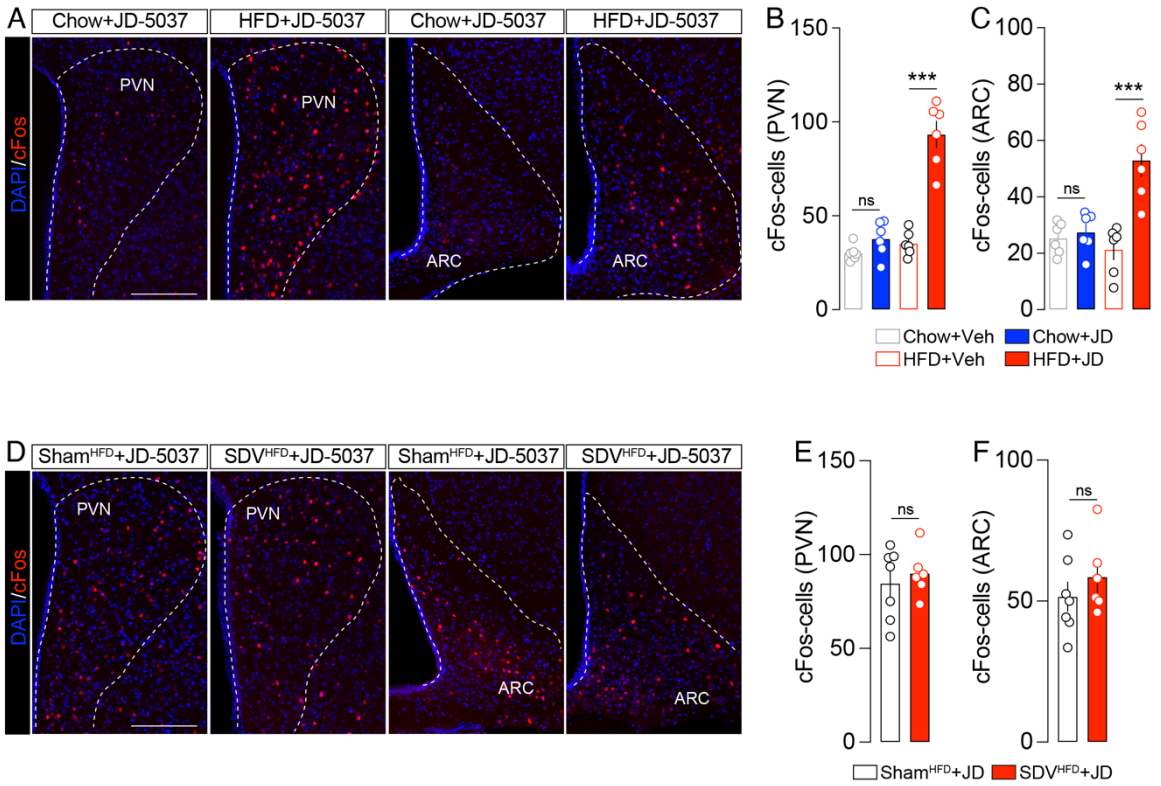

Figure 6: Inhibition of peripheral CB1R leads to the activation of hypothalamic nuclei via a vagus nerve-independent mechanism. (**A**) Immunofluorescence detection of cFos in the paraventricular nucleus (PVN) and arcuate nucleus (ARC) of the hypothalamus of chow- and HFD-mice administered with JD-5037 (3 mg/kg). Quantifications of cFos-positive cells in the PVN (**B**) and ARC (**C**) of chow- and HFD-mice administered with vehicle or JD-5037 (3 mg/kg) (n=6 mice/group). (**D**) Immunofluorescence detection and quantifications (**E, F**) of cFos-positive cells in the PVN and ARC of Sham^{HFD}- and SDV^{HFD}-mice administered with JD-5037 (3 mg/kg) (n=6-7 mice/group). Scale bars: 150 µm. Statistics: One-way ANOVA followed by a Bonferroni *post hoc* test (B, C panels) or Student's t-test (E, F panels), ***p<0.001 for specific comparisons.